CHAPTER 7

Automated system for diagnostics of shot state parameters based on features of different physical nature

Volodymyr Demydenko
Yevhenii Dobrynin
Oleksii Maksymov
Ruslan Riaboshapka

Abstract

This chapter presents an integrated approach to the verification and diagnostic assessment of an artillery shot based on the joint analysis of acoustic signals and optoelectronic observations.

The proposed method combines physical modeling of ballistic and muzzle wave formation with data processing techniques aimed at extracting informative parameters from heterogeneous measurement channels.

Particular attention is paid to the synchronization of acoustic records with video-based observations of the muzzle blast dynamics, which allows improving the reliability of determining key shot characteristics. A unified framework for representing measured and tabulated parameters is introduced, enabling consistent comparison of experimental data with reference values.

The chapter discusses the principles of feature selection, the formation of diagnostic indicators, and the interpretation of results under conditions of incomplete or uncertain information.

The obtained results demonstrate that the integration of acoustic and visual data provides additional robustness of diagnostic conclusions and can be used to enhance automated monitoring systems for artillery equipment.

The proposed approach may be applied to the development of advanced verification procedures and to the improvement of decision-support tools in complex technical systems where direct measurement of internal processes is limited.

Keywords

Acoustic diagnostics, muzzle blast dynamics, artillery shot verification, optoelectronic monitoring, parameter estimation, signal processing.

 DOI: 10.21303/978-9908-8450-1-2.ch7

7.1 Introduction

The development of modern diagnostic and monitoring methods for complex technical systems increasingly relies on the integration of heterogeneous measurement channels and advanced data processing techniques. In the case of artillery systems, the analysis of acoustic fields, optical observations, and indirect physical indicators makes it possible to obtain informative features describing the state of the firing process and the technical condition of the weapon. Such an approach requires the application of unified mathematical models capable of describing nonlinear dynamic phenomena under conditions of uncertainty and incomplete measurement information [1, 2].

A significant number of recent studies demonstrate that the effective analysis of dynamic physical processes is based on approximation models, inverse problem formulations, and analytical representations of system parameters. In particular, approaches involving sets of linear differential models, analytical solutions of Riccati-type equations, and parameter identification techniques provide a flexible framework for describing complex processes of various physical nature, including ballistic, acoustic, and physicochemical phenomena [3–7]. These methods enable the reduction of computational complexity while preserving sufficient accuracy for practical applications.

Another important aspect of modern research is the transferability of modeling principles between different scientific domains. Methods originally developed for describing combustion processes, pyrolysis of materials, or energy transformations in reactive systems can be successfully adapted for analyzing measurement signals obtained during artillery firing. The use of library-based modeling approaches, adaptive process representations, and models of systems with variable composition demonstrates the universality of mathematical tools for interpreting experimental data and constructing diagnostic indicators [8–10].

Within this context, acoustic and optoelectronic data acquired during a shot can be interpreted as manifestations of coupled dynamic processes governed by the physics of gas expansion, wave propagation, and interaction of combustion products with the environment. Physical models of acoustic wave formation and studies of ballistic processes provide the theoretical foundation for extracting informative parameters from measurement records and for constructing classification or estimation procedures [1, 5, 10].

Therefore, the development of integrated diagnostic approaches based on heterogeneous physical fields represents a relevant scientific and applied task. The combination of mathematical modeling, signal processing, and experimental analysis creates prerequisites for improving the reliability of state assessment methods and for extending the functionality of automated diagnostic systems operating under real-world conditions [1–10].

The present chapter focuses on the development of a diagnostic framework for artillery shot verification based on the combined analysis of acoustic measurements and video recordings of muzzle blast dynamics. Particular attention is given to the formation of informative indicators derived from heterogeneous data sources and to the harmonization of measured and reference parameters within a unified analytical scheme. The proposed approach aims to improve the reliability of identifying shot characteristics under real operating conditions, where direct observation of internal ballistic processes is limited. The following sections describe the structure of the experimental data, the principles of parameter representation, and the procedures used for extracting diagnostic features from synchronized acoustic and visual records.

7.2 Methods for detection of diagnostic features of shot state parameters

The system of automated diagnostics of artillery shot state parameters is based on two independent methods that use diagnostic features of different physical nature. In the first diagnostic channel, the features are formed by acoustic waves of two types – muzzle and ballistic waves. In the second diagnostic channel, the features are formed by the presence of free carbon in the propellant gases during the shot. The general scheme of the automated diagnostic system is shown in **Fig. 7.1**.

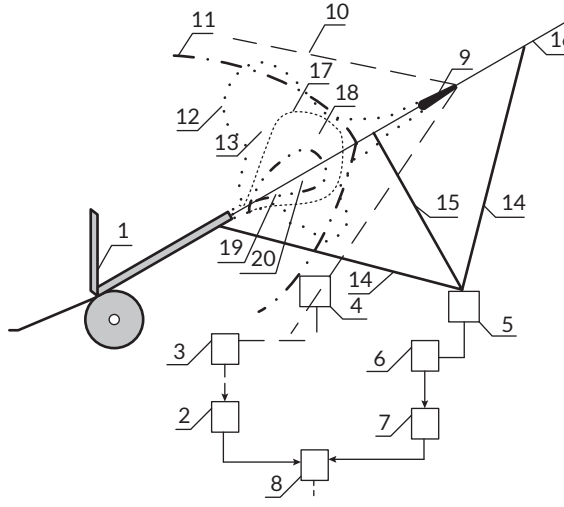

Fig. 7.1 General scheme of the automated system for diagnostics of shot state parameters

The first channel registers acoustic fields that arise during the projectile motion after leaving the barrel bore. The diagnostic characteristic in this case is the projectile velocity. The improved diagnostic method of the first independent channel, which is based on the difference between the velocities of the muzzle and ballistic waves, is implemented according to the sequence given below.

The detection of the diagnostic feature of the shot state based on projectile velocity V_p^{meas} is performed as follows:

Step 1. The artillery gun 1 is loaded with a projectile with a specified propellant charge which, according to the firing tables, should provide the initial projectile velocity V_p^{tab}.

Step 2. A microphone 4 is placed on the firing line at a known distance from gun 1; it is connected to the analog-to-digital converter equipment 3 and to computer 2. The microphone 4 is positioned along the firing direction line 16 to register the ballistic wave 10 and the muzzle wave 11. Subsequently, the velocity of the muzzle wave from gun 1 to microphone 4 is determined taking into account the averaged atmospheric parameters near gun 1 and microphone 4.

Step 3. After the shot from gun 1, along the firing direction 16, the microphone 4 records the signal of the ballistic wave 10 from the projectile 9 moving along the firing direction line 16; at this moment of time t_{bw} the muzzle wave 11 is located at some distance from gun 1, and after a time t_{mw} the microphone 4 registers the spectrum of the muzzle wave 11 generated by the shot of gun 1.

Step 4. From the obtained current signal spectra, the amplitude and duration of the ballistic wave signal 10 are determined, as well as the amplitude and the duration of the first half-period of the muzzle wave 11 at the microphone location at a known distance from gun 1.

Step 5. The signals from microphone 4 are transmitted to the analog-to-digital converter 3 and then to computer 2, where the signals are transformed into the spectral domain. In the spectral domain, the spectral energy density of the signal is determined over frequency.

Step 6. For the obtained spectra, the width at the 0.707 level is fixed for the ballistic wave signal 10, and the central frequency (frequency of maximum) is determined for the muzzle wave 11.

Step 7. The propagation time of the muzzle wave t_{bw} 11 from gun 1 to microphone 4 is determined using the known distance between gun 1 and microphone 4 and the calculated propagation velocity of the muzzle wave 11.

Step 8. The propagation time of the ballistic wave t_{bw} is determined as the difference between the propagation time of the muzzle wave and the time interval between the registration of the ballistic and muzzle waves by the microphone.

Step 9. The velocity of the ballistic wave 10, which corresponds to the actual projectile velocity V_p^{meas}, is determined from the time t_{bw} of its registration by microphone 4 or using the known distance between gun 1 and microphone 4.

Step 10. The measured projectile velocity V_p^{meas} is compared with the tabulated projectile velocity V_p^{tab}, and the diagnostic feature is obtained based on the change in projectile velocity.

The possibility of implementing the second channel is considered in [5]. In this approach, the formation of free carbon is proposed as a diagnostic characteristic. The suggested diagnostic method of the second independent channel is based on the appearance of free carbon in the muzzle blast of powder gases, which expand to atmospheric pressure after the moment when the projectile leaves the gun barrel, and it is implemented in the following way.

Detection of the diagnostic feature by the presence of free carbon is performed according to the following sequence:

Step 1. The artillery gun 1 is positioned so that the muzzle section of the gun barrel is perpendicular to line 15. Along this line a digital high-frequency wide-angle video camera 5 is installed, which is connected to a personal computer 6 where a software package for video stream processing is loaded.

Step 2. The video camera 5 is switched on and recording starts in the visible and infrared ranges. After the shot, the digital video stream is transmitted in real time to the personal computer 6 with the processing software.

Step 3. Video recording is stopped and the video camera 5 is switched off after the projectile 9 passes the boundary of the camera field of view 14.

Step 4. The video stream is converted into a sequence of frames using the personal computer with the software package 6, and this sequence is transferred to the analysis module 7.

Step 5. Each frame is analyzed in the analysis module 7 in order to detect the image of projectile 9 in the frame. The time frames containing the projectile image are selected into a separate array starting from the moment when the projectile image separates from the muzzle edge of gun 1 up to the moment when the projectile image is no longer present.

Step 6. For each time frame further processing is performed if the necessary data for calculation are available.

Step 7. In the frame image the position of the center of mass of projectile 9 is determined, and at this point the coefficient of geometric recalculation of linear dimensions is obtained using the a priori known dimensions of the projectile (diameter and length).

Step 8. The linear distance between the center of mass of projectile 9 and the muzzle section of the gun barrel is determined from the image of the muzzle section

of gun 1 to the point of the projectile center of mass, taking into account the geometric recalculation coefficient, and the averaged instantaneous velocity of projectile 9 on this segment is evaluated V_p^{avg}.

Step 9. A statistically reliable initial linear velocity of projectile 9 V_p^{meas} is calculated after analysis of all time frames.

Step 10. The length of curved line 19 – the boundary between the projection of the free carbon surface and the powder gases 20, when present, which exit the gun barrel into the atmosphere with excessive pressure during the observation time interval – is determined, and time series of lengths 19 and areas 20 are formed; these characteristics constitute a diagnostic feature of the shot state parameters.

Step 11. The length of curved line 17 – the boundary between the projection of surface 18 of powder gases and free carbon at the stage of instantaneous ignition with pressure higher than atmospheric and the surrounding atmosphere – is determined over the observation interval, forming a muzzle shock wave in the atmosphere and generating time series of lengths 17 and areas 18.

Step 12. The length of curved line 12 – the boundary between the projection of the burned powder gas surface 13 with atmospheric pressure and the atmosphere, formed by the volume of the powder exhaust and the surrounding air during the observation interval – is determined, and time series of lengths 12 and areas 13 are formed.

Step 13. Based on the formed time series of lengths and areas, pressure change gradients are evaluated; the absence of a pressure gradient indicates the formation of a curved boundary line between the projection of powder gases and the atmosphere, which characterizes the transition between stages of the muzzle blast: free carbon with hot powder gases without mixture ignition; expansion of the mixture in the air atmosphere with ignition and afterburning; and stabilization of the pressure of powder gases that have burned in the atmospheric air.

Step 14. Using personal computer 6 with the software complex and the calculation-analysis module 7, the current volume of powder gases and their temperature are determined for each time frame; the temperature is measured by the digital high-frequency wide-angle video camera operating in the visible and infrared ranges 5, and the current pressure of powder gases at the front of the muzzle shock wave is calculated.

Step 15. The volume of burned powder gases at atmospheric pressure is determined along curved line 12 – the boundary between the projection of the flame surface of burned powder gases 13 and the atmosphere.

Thus, two methods are proposed that are based on measurements of physical fields of different nature, but describe one process – the artillery shot.

7.3 Muzzle blast video recording

The muzzle blast during firing from modern large-caliber weapons has a complex three-lobed shape (**Fig. 7.2**).

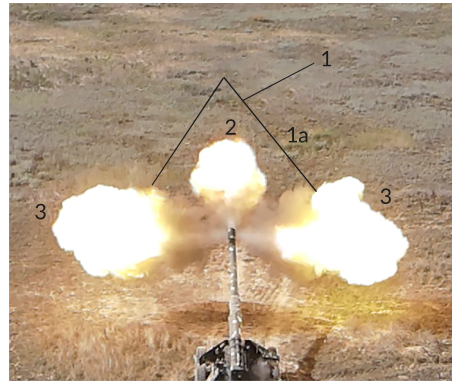

Fig. 7.2 Muzzle blast formed during a shot from a 152-mm gun: 1 – projectile; 1a – mach cone accompanying the projectile; 2 – frontal exhaust of powder gases; 3 – lateral exhausts of powder gases through the compensator (muzzle brake) openings of the gun

The frontal exhaust of powder gases is associated with their eruption from the barrel, while the left and right lateral exhausts are formed when the combustion products exit through the openings of the gun's compensator. For diagnosing the barrel's condition, it is important to obtain the maximum amount of information on the dynamics of muzzle blast development. This is achieved by high-speed video recording of the muzzle blast from different angles.

The field experiment was carried out during training firing of 152-mm towed guns. Shots were performed with two guns: Gun No. 1 – with a barrel of minimal wear (91 shots); Gun No. 2 – with a barrel of significant wear (1968 shots). During subsequent firing, physical fields were recorded from 59 shots: 34 from Gun No. 1 and 25 from Gun No. 2.

The scheme of video recording during firing is shown in **Fig. 7.3**.

In the scheme (**Fig. 7.3**), the origin *O* is aligned with the muzzle of the gun barrel (1). The *Ox* axis coincides with the firing direction. The projectile (2), after leaving the muzzle, moves along its trajectory. Upon the projectile's exit, frontal (3) and lateral (4, 5) muzzle blasts are formed. At a distance of $l_1 = 60–100$ m on a line perpendicular to the firing direction, a ground-based high-speed video system is installed.

The video system consists of a visible-range camera (6) and an infrared (IR) camera (7). This setup (6, 7) is used to record the dynamics of the muzzle blast development from a ground-level side view. A high-speed camera (8) is positioned along an inclined line in the vertical plane at a distance of $l_2 = 60–100$ m. During the experiment, camera (8) was mounted on a hovering unmanned aerial vehicle. Camera (8) records the muzzle blast from a vertical perspective. The video streams from cameras (6–8) are synchronized and transmitted via radio and wired channels to a computing workstation.

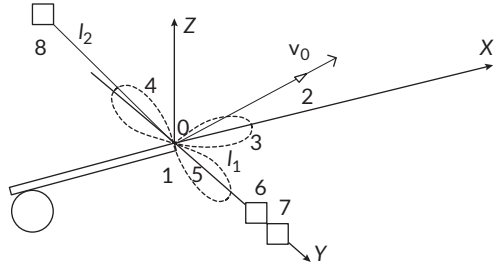

Fig. 7.3 Scheme of muzzle blast video recording during a shot: 1 – gun barrel; 2 – projectile; 3 – frontal exhaust; 4, 5 – left and right lateral exhausts; 6 – ground-based visible-range video camera for recording the horizontal side view; 7 – infrared-range video camera; 8 – visible-range video camera for recording the vertical view

In the experiment, the following equipment was used:

1) infrared camera: high-speed MWIR Science-Grade Camera FLIR X6980; resolution 640 × 512 px; frame rate up to 1004 Hz; standard ND2 filter used: (250...2000)°C; dynamic range 14 bit; real-time connection via Ethernet port;

2) visible spectrum cameras: high-speed FASTCAM MINI WX camera, shockwave-protected; resolution 1920 × 1080 px; frame rate from 240 Hz; linear imaging (without lens or perspective distortions); real-time video signal connection;

3) workstation for processing recorded data: GPU: RTX 3080; CPU: 4.5 GHz, 12 cores; storage: SSD 4 TB M.2 NVME; RAM: 64 GB; OS: Windows 10.

During all shots, acoustic fields – ballistic and muzzle waves – were additionally recorded. Since the methods of their registration are discussed in detail in works [2, 11, 12], they are not covered in this section.

Fig. 7.4 shows consecutive frames of the muzzle blast dynamics in a top vertical view.

Analysis of consecutive frames reveals significant differences between muzzle blasts from worn and serviceable barrels. This allows considering the possibility of creating an automatic barrel condition classifier based on video data.

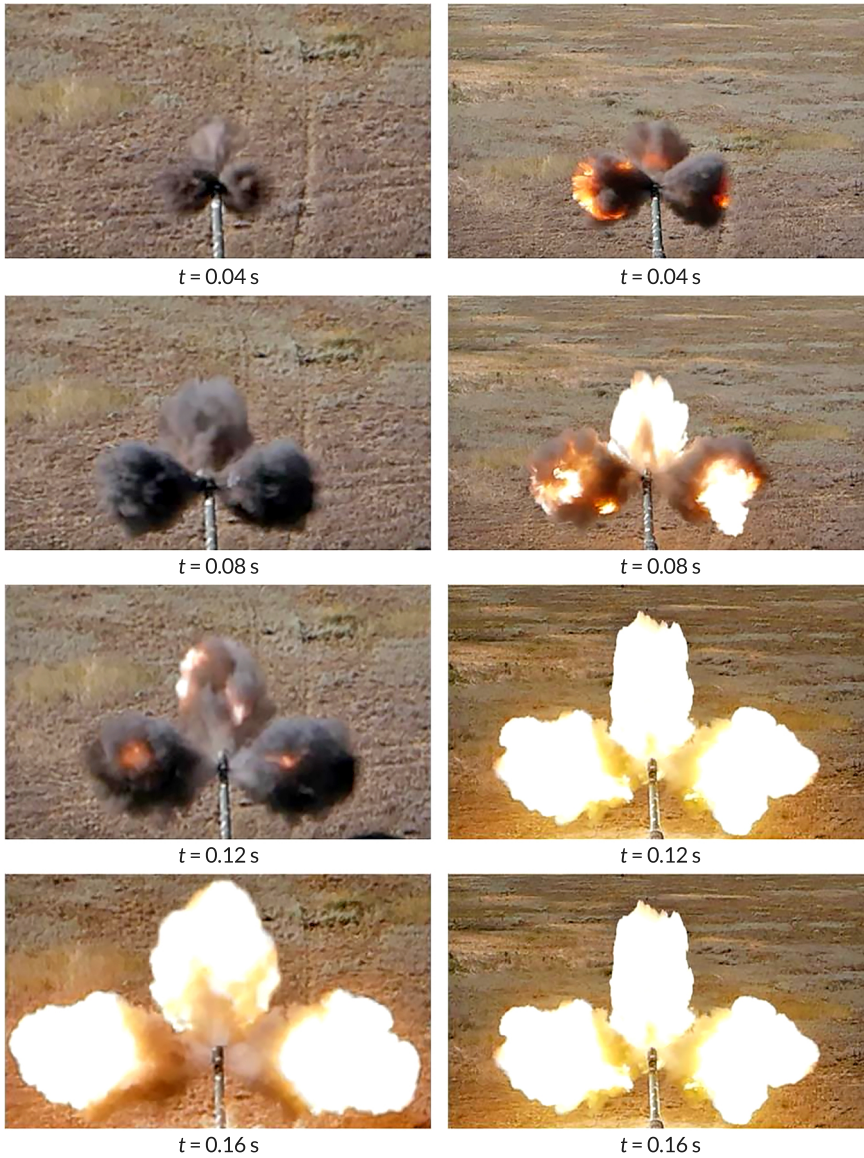

Fig. 7.4 Sequential frames of the muzzle blast development dynamics in the upper vertical view: *a* – shot from a worn barrel; *b* – shot from a non-worn barrel

7.4 Method for forming diagnostic features of the muzzle blast based on video analysis

The procedure for forming diagnostic features of the muzzle blast based on video analysis is implemented as follows:

Step 1. Synchronous video recording is performed with all cameras, and shortly after, the shot is fired. Two visible-spectrum video streams from cameras (6) – file_1 (horizontal view) and (8) – file_2 (vertical view), as well as the IR stream from camera (7) – file_1ir, are transmitted to the computer.

Step 2. The video streams (file_1), (file_2), and (file_1ir) are converted into a synchronized sequence of frames with discrete time stamps.

Step 3. Each frame is analyzed to locate the projectile in the image. An array of frames containing the projectile is then formed – from the moment it separates from the barrel muzzle or leaves the powder-gas cloud until it disappears from the frame.

Step 4. For each frame, if IR stream data (file_1ir) is available, the projection of the temperature field is analyzed. The frames from all three video streams are synchronized and form two geometric projections of the muzzle blast, as well as, if data is available, the distribution of the average temperature field.

Step 5. On the side-view frame, the position of the projectile's center of mass is determined. At this point, a geometric scaling coefficient for linear dimensions is calculated based on the a priori known projectile dimensions (diameter and length).

Step 6. The actual distance between the center of mass of the projectile and the barrel muzzle is determined, taking into account the geometric conversion factor. The average velocity of the projectile along this segment is then calculated.

Step 7. Based on the analysis of all frames, the statistically reliable initial velocity of the projectile is determined immediately after leaving the barrel V_0^{val}.

Step 8. From the IR frames, the length of the boundary between the projections of free carbon, gunpowder gases, and the atmosphere is determined, as well as the area of this region, if present.

Step 9. Using frames from cameras (6) and (8), the areas of the muzzle flash projections are determined, based on which the current volume of the muzzle flash is calculated.

Step 10. For each time frame, the current pressure of the gunpowder gases at the front of the muzzle shock wave is calculated. The current gas pressure of the muzzle flash is determined from the average temperature, the current gas volume, and the characteristics of the gas contained in the muzzle flash. Reaching atmospheric pressure indicates the disappearance of the shock wave as a diagnostic feature.

Step 11. Analysis of the obtained calculation vectors. Two vectors are formed during the analysis: pressure and temperature of the muzzle flash gases. The pressure vector shows a monotonic decrease to the atmospheric value. The temperature vector may show a monotonic decrease, a jump followed by decline, or a stabilization section.

The presence of free carbon is indicated by a temperature jump or stabilization, explained by additional oxidation during mixing with atmospheric oxygen. This temperature property of the muzzle gas volume confirms that during its expansion and mixing with atmospheric oxygen, additional oxidation of free carbon occurs, releasing extra energy, which produces the described temperature characteristic.

Fig. 7.5 shows a diagram of the processing of the video information stream corresponding to the described methodology.

Below are the key operations of the methodology that require illustration. **Fig. 7.6** shows a condensed video sequence of combined frames from the vertical and side views, highlighting the key moments of the projectile exit and the development of the muzzle blast.

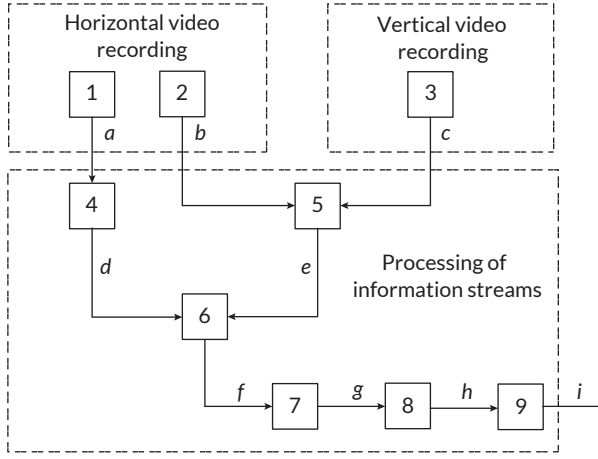

Fig. 7.5. Diagram of the processing of video information streams: 1 – IR spectrum camera; 2 – side-view camera; 3 – vertical-view camera; 4 – preliminary processing of IR video stream; 5 – preliminary processing of visible-spectrum video stream; 6 – frame image alignment; 7 – detection of analysis regions in the frame; 8 – detection of the IR spectrum image of the muzzle gas region in the frame; 9 – calculation of the perimeter and area of the muzzle gas volume; *a* – IR spectrum video stream; *b* – visible-spectrum video stream; *c* – visible-spectrum video stream; *d* – normalized set of IR spectrum frame images; *e* – normalized set of visible-spectrum frame images; *f* – time-based set array (time, frame, position); *g* – array of numerical characteristics; *h* – array of numerical characteristics; *i* – two formed vectors of characteristics

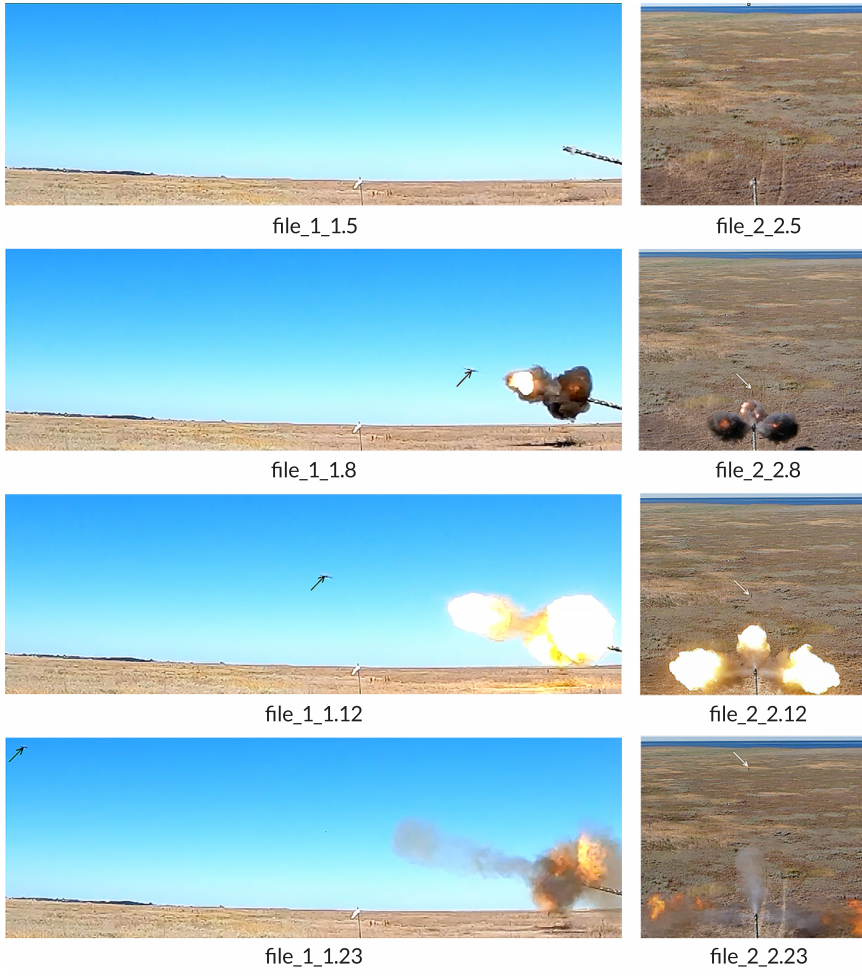

Fig. 7.6 Typical sequence of overlaid frames (file_1, file_2) from vertical and side views. Four key moments are shown: the first frame (5), intermediate frames (8, 12), and the last frame (23), illustrating the projectile flight and the development of the muzzle blast (the projectile is indicated by arrows)

After converting the video streams (file_1) and (file_2) into frame sequences, for each pair of frames file_1_1.i and file_2_2.i, filtering, extraction of closed contours, and determination of their geometric dimensions relative to the baseline size –

the outer diameter of the gun barrel – were performed using the OpenCV library. From the processed frame of camera file_1_1.i, the diameter D_1 and length L_1 of the frontal muzzle blast were determined. Additionally, the diameter D_2 of the left-side muzzle blast through the muzzle brake was measured. It was assumed that the diameters of the right and left side blasts are equal in the current frame. From the processed frame of the vertical camera file_2_2.i, the lengths L_2 of the left-side muzzle blast and L_3 of the right-side muzzle blast from the gun with the muzzle brake were determined (**Fig. 7.7**).

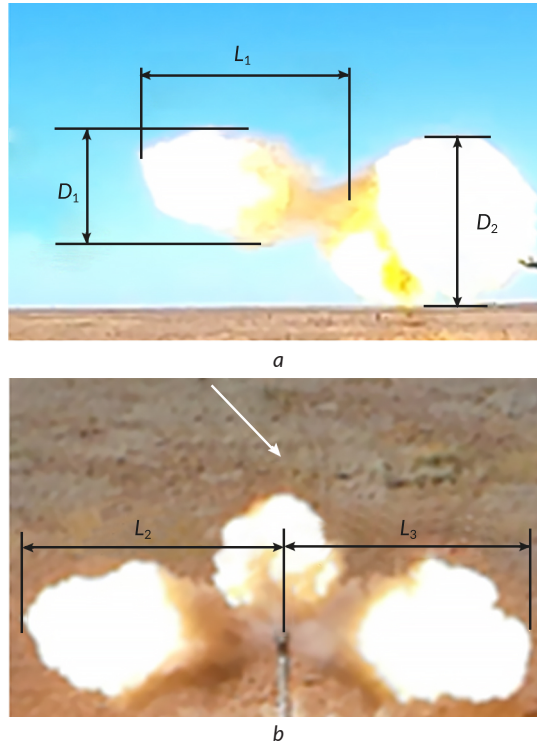

Fig. 7.7 Determination of muzzle gas dimensions:
a – determination of geometric dimensions from the side-view camera;
b – determination of geometric dimensions from the vertical-view camera

It was assumed that the obtained geometric dimensions of the "lobes" of the muzzle blast correspond to bodies in the form of rotational ellipsoids. In this case,

the total current volume of the muzzle blast was determined as the sum of the volumes of three geometric bodies

$$V_i = \frac{4}{3}\pi(L_1 D_1^2 + L_2 D_2^2 + L_3 D_3^2).$$

The current pressure P_i in the gas volume V_i with an average temperature T_i is determined based on the ideal gas law, using the Mendeleev-Clapeyron equation

$$P_i V_i = \frac{m}{M} R T_i.$$

This assumption is acceptable for the considered stage of the muzzle blast expansion, when the powder gases rapidly expand into the atmosphere and the pressure decreases to values close to atmospheric pressure. Under these conditions, the deviation of the gas mixture behavior from the ideal gas model does not significantly affect the calculated pressure estimates.

While the gas expands from the barrel into the air atmosphere after exiting the muzzle, it is assumed that no chemical reactions occur in the muzzle-blast gas; that is, the gas mixture maintains a constant composition. For this reason, the molar mass M of the gas mixture in the system "charging chamber – barrel bore – muzzle blast" is constant. Accordingly, the mass m of the gas mixture contained within the entire muzzle system ("charging chamber – barrel bore – muzzle blast") remains unchanged. The universal gas constant is also constant. The product $(m/M)R$ is therefore treated as a constant value for the calculations, and its detailed evaluation is presented in [5]. It should be noted that for each shot this product has its own value and depends on the propellant charge, the powder type, its granulometric properties, and the wear condition of the barrel system.

The temperature T_i is determined from horizontal recording using an infrared video camera that captures temperature data in file (file_1ir). Based on the correspondence between video frames file_1_1.i and file_1_1ir.i, the property of the measured temperature is extended to the entire portion of the muzzle-blast gases of the given fragment.

Fig. 7.8 presents the results of joint processing of frames from the video sequences (file_1), (file_2), (file_1ir), demonstrating changes in gas pressure and temperature within the muzzle blast. **Fig. 7.8** was obtained by processing the video sequence shown in **Fig. 7.6** (the left column corresponds to a shot from a barrel with high wear, the right column corresponds to a shot from a barrel without wear).

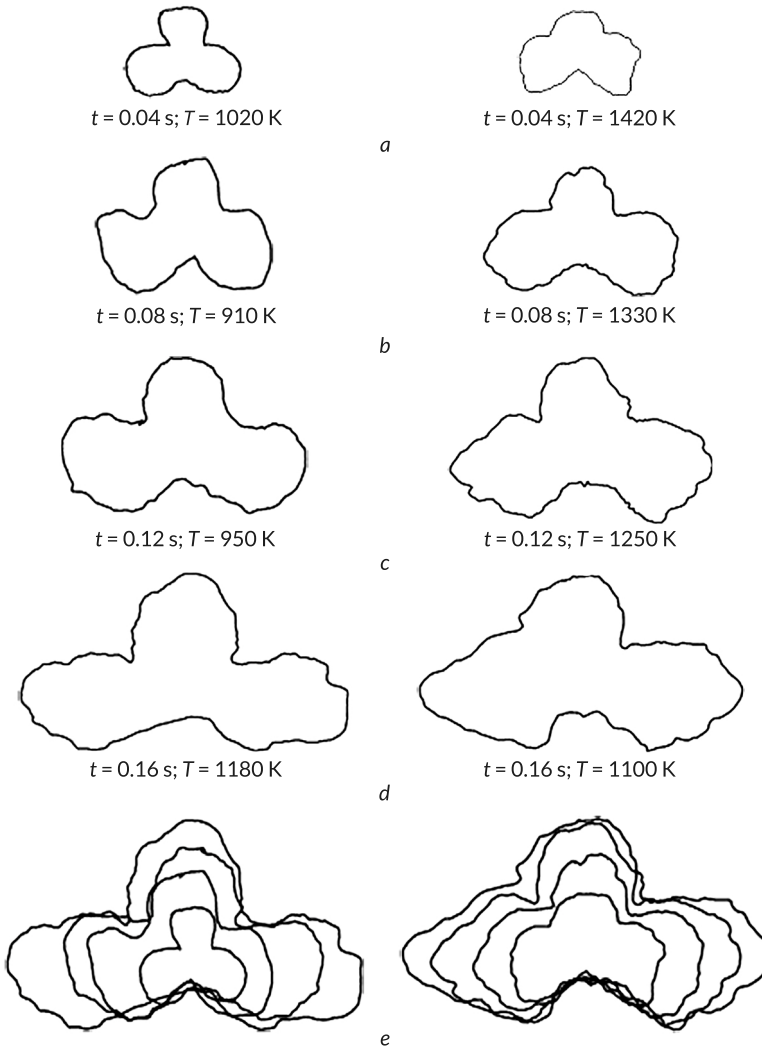

Fig. 7.8 Results of joint processing of frames from the video sequences (file_1), (file_2), (file_1ir), demonstrating changes in gas pressure and temperature in the muzzle blast (rows *a*, *b*, *c*, *d*) for two different barrel conditions; row *e* shows the gas pressure gradient in the muzzle blast. In the first case, the shock wave transformed into an acoustic wave within the time interval from 0.08 s to 0.12 s after projectile exit, whereas in the second case – from the beginning of the exit up to 0.04 s

7.5 Selection of informative parameters for classification of barrel condition based on analysis of video recordings of muzzle blast dynamics

By analogy with classification based on acoustic fields, for classification using video recordings of the muzzle blast the main objective of video analysis is the selection of informative features that distinguish a worn barrel from a defect-free one. Analysis of the obtained video sequences made it possible to form a set of informative parameters (IP) used for binary classification of defect-free and worn barrels.

The following parameters were used as the main classification features:

– $F_{1,i}^{vid}$ – the perimeter of the contour bounding the muzzle-blast region in the frame recorded at time t s after the shot – L_t; the perimeter was calculated for time instants t = 0.04 s, 0.08 s, 0.12 s, 0.16 s, thus forming four informative parameters (IP): $F_{1,0.04}^{vid}$, $F_{1,0.08}^{vid}$, $F_{1,0.12}^{vid}$, $F_{1,0.16}^{vid}$;

– $F_{2,i}^{vid}$ – the projection area of a part of the muzzle blast onto the image plane at time t s after the shot – S_t; it was calculated for the same time instants, forming four additional informative parameters (IP): $F_{2,0.04}^{vid5}, F_{2,0.08}^{vid6}, F_{2,0.12}^{vid7}, F_{2,0.16}^{vid8}$.

These time instants correspond to characteristic stages of muzzle blast development identified during the preliminary analysis of the video sequences. The selected moments provide stable measurements of geometric parameters while keeping the dimensionality of the feature vector limited.

The volume of a part of the muzzle blast at time instants t = 0.04 s, 0.08 s, 0.12 s, 0.16 s was used as informative parameters from the 9th to the 12th:

$$F_{3,0.04}^{vid9}, F_{3,0.08}^{vid10}, F_{3,0.12}^{vid11}, F_{3,0.16}^{vid12}.$$

Since previous experiments revealed differences in the dynamics of changes in the volume of a part of the muzzle blast, the following derived features were formed:

– $F_{4,40-120}^{vid13}$ – estimation of the growth rate of the volume of a part of the muzzle blast in the time interval from 40 ms to 120 ms;

– $F_{4,120-160}^{vid14}$ – estimation of the growth rate of the volume of a part of the muzzle blast in the time interval from 120 ms to 160 ms.

These features were calculated as follows:

$$V_{40-120}^{meas} = \frac{V_{120} - V_{40}}{80},$$

$$V_{120-160}^{meas} = \frac{V_{160} - V_{120}}{40}.$$

For all recorded shots, 14 informative parameters were calculated.

Since the SVM (support vector machine) classifier [12] proved effective for classifying barrel condition based on ballistic and muzzle acoustic waves, this classifier was also tested for assessing barrel condition from muzzle flash video recordings. Unlike [12], in this case a more efficient variant of SVM was chosen – the least squares support vector machines (LSSVM) method [13]. LSSVM is a modified SVM approach that reduces the problem to solving linear systems of equations, effectively transforming it into a linear programming task, whereas the classical SVM method requires solving a quadratic programming problem. The LSSVM method significantly reduces computation time while maintaining classification quality. Its use also allows for a substantial reduction (by 2–4 times) in the required training dataset [14]. The LSSVM method is implemented as a MATLAB Toolbox [15].

For the binary classification of barrel condition from muzzle flash video recordings, feature vectors were calculated for 59 recordings obtained during the experiment. The standard procedure of training, tuning, and testing the LSSVM classifier [13, 14] was then performed. All the above-mentioned informative features were normalized to the interval [0, 1]. The training dataset for tuning and training the classifier consisted of feature vectors from 30 randomly selected recordings. After training, the classifier's performance was evaluated using a test dataset consisting of feature vectors from 25 recordings, 13 of which were from shots with a defect-free barrel, and 12 from a worn barrel. The remaining four recordings were not included in the training or test subsets and were reserved as additional data for verifying the stability of the obtained results.

Until now, classification quality was quantified using a single metric – accuracy, defined as the ratio of correctly classified objects to the total number of objects [16]. This measure alone is not sufficient. The classification logic and results are presented in **Table 7.1**. Columns 2 and 3 of **Table 7.1** indicate the true classes corresponding to the barrel condition. The rows of **Table 7.1** show the classifier's decisions, indicating to which of the two classes the classifier assigned each shot. Each cell at the intersection of a row and a column contains the number of true or false classification outcomes.

Since the primary goal of classification is to detect barrel condition, the state "Barrel truly worn" is considered the true positive condition, whereas the opposite state, "Barrel truly operational", is considered the true negative condition. Classifier outputs may therefore be: "Barrel worn", which is a true positive decision, and "Barrel operational", which is a true negative decision. The meaning of false positive and false negative decisions is evident from **Table 7.1**. The corresponding

cells in **Table 7.1** show the quantitative classification results for the examined dataset.

Table 7.1 Logic of barrel condition classification results

Barrel condition	True positive condition	True negative condition
Classifier decision	"Barrel actually worn"	"Barrel actually serviceable"
Classified as: "barrel worn"	True positives (*TP*)	False negatives (*FN*)
Classified as: "barrel serviceable"	False positives (*FP*)	True negatives (*TN*)

The classification quality was evaluated using three metrics.

The first metric is the Type I classification error, defined as the proportion of classifier decisions that identify a worn barrel as serviceable

$$F_1 = \frac{FN}{N_{def}},$$

where N_{def} – the actual number of worn barrels.

The second metric, Type II classification error, is defined as the proportion of classifier decisions that identify a serviceable barrel as worn

$$F_2 = \frac{FP}{N_{ok}},$$

where N_{ok} – the actual number of serviceable barrels.

Undoubtedly, a Type I error is more critical in terms of consequences, but in combat conditions, a Type II error also has operational impact, as it leads to removing a serviceable gun from the field and transporting it to a technical unit for diagnostics.

Therefore, a third metric is introduced, which serves as a generalized measure of classification quality and indicates the probability of error-free barrel condition classification

$$P_0 = 1 - (F_1 + F_2).$$

The summarized results of barrel condition classification based on different physical fields and their combinations are presented in **Table 7.2**.

Table 7.2 Comparative results of barrel condition classification based on different physical fields of the shot

Indicators	Classification results based on analysis				
	BW	MW	BW + MW	MDV	BW + MW + MDV
P_0 – probability of correct classification	0.29	0.44	0.60	0.52	0.77
F_1 – Type I error	0.33	0.25	0.17	0.33	0.08
F_2 – Type II error	0.38	0.31	0.23	0.15	0.15

Note: MDV – video recording of muzzle blast dynamics

7.6 Investigation of classifier generality

The practical interest lies in exploring the possibility of classifying barrel condition based on different physical fields and their combination. Below, the classification results for the acoustic fields of ballistic and muzzle waves and their combination, summarized in **Table 7.2**, are analyzed. For this purpose, the informative features used for training and testing the classifier are those detailed in [2, 11, 12]. The training and test samples coincide with those used for classification from the video recording of muzzle blast dynamics.

To assess the generality of the approach, classification was performed using the acoustic field of the ballistic wave, the muzzle wave, their combination, as well as in combination with the MDV.

The results presented in **Table 7.2** show a significant increase in classification accuracy when all physical fields of the shot are used in combination.

This effect can be explained by the fact that the acoustic and video channels are based on physical fields of different nature and are affected by different sources of measurement uncertainty. Therefore, their classification errors are only partially correlated, and the joint use of these channels increases the robustness of the diagnostic system.

The highest performance is achieved when combining the informative features of the acoustic fields with the MDV.

The automated system for diagnosing shot parameters (**Fig. 7.9**) consists of hardware and software components. The hardware component includes three elements: I – a set of technical means for measuring the acoustic field generated by muzzle and ballistic waves; II – a set of technical means for horizontal and vertical video recording of muzzle gases; IV – a mobile device for displaying the obtained shot parameter results within the automated diagnostic system (**Fig. 7.9**).

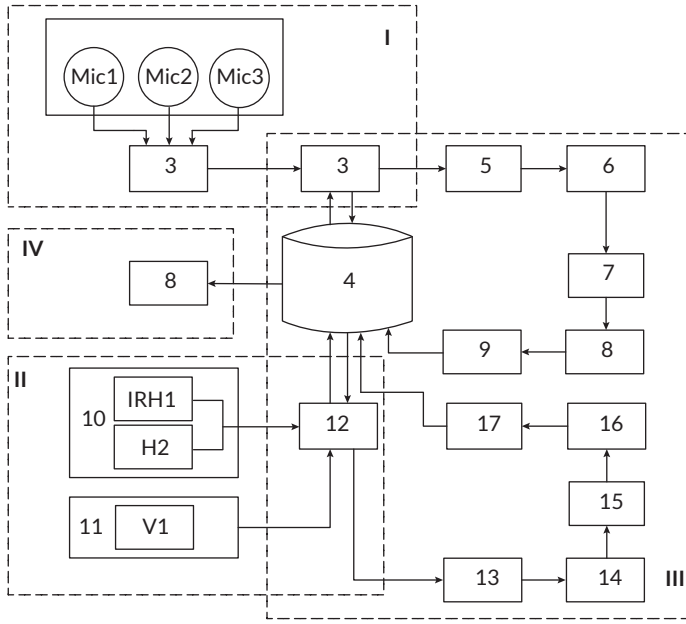

Fig. 7.9 Diagram of the automated system for diagnosing shot parameter states

The subsequent processing of the collected information is performed by the software component III, presented as the overall structure for processing information obtained from various physical fields during the shot (**Fig. 7.9**). The software component includes: an integrated database; programs for processing recordings, signals, images, and video sequences, as well as for extracting and accumulating informative features; SVM and LSSVM classifiers:

– I – a set of technical means providing measurement of the acoustic field generated by muzzle and ballistic waves;

– II – a set of technical means providing horizontal and vertical video recording of the muzzle gas plume;

– III – general structure of the software component for digital processing of information obtained from various physical fields during the shot;

– IV – mobile device for displaying results obtained in the automated system for diagnosing shot parameter states;

– 1 – group of measurement microphones for acoustic wave characteristics.

– 2 – multichannel 16-bit ADC;

– 3 – field computer for calculating acoustic wave parameters;
– 4 – integrated database;
– 5 – recording processing (extraction of ballistic and muzzle wave signals);
– 6 – recording processing (extraction of sets of informative features of the acoustic field);
– 7 – formation and training of the SVM acoustic field classifier;
– 8 – shot classification using acoustic diagnostic features;
– 9 – classification result of the shot based on the acoustic field;
– 10 – group of horizontal video cameras (IRH1 – infrared horizontal, H2 – horizontal);
– 11 – vertical video camera V1;
– 12 – field computer for processing muzzle gas video images;
– 13 – video recording processing;
– 14 – processing of individual image frames;
– 15 – formation and training of the LSSVM classifier for muzzle gas images;
– 16 – shot classification using diagnostic features obtained from the muzzle gas;
– 17 – classification result of the shot based on processing of muzzle gas images;
– 18 – classification result of the shot based on the combination of muzzle gas video and acoustic shot fields.

A field experiment was conducted using a set of technical means for recording muzzle blast and a system for measuring the acoustic field generated during training firings of towed guns. The hardware setup for the gun position included three measurement condenser microphones – Rode NT1-A, Rode NT-USB, and DPA 4062-OC – connected to a MacBook Pro 15 via a 16-bit, multi-channel ADC TASCAM 102i. The specifications of the measurement microphones were as follows: frequency range 20 Hz–20 kHz; signal-to-noise ratio 81 dB; sensitivity 32 dB relative to 1 V/Pa; dynamic range 132 dB.

7.7 Conclusions

A field experiment was conducted to record the muzzle blast of propellant gases accompanying gunfire using high-speed cameras in both visible and infrared ranges from multiple observation angles. The experiment revealed significant differences in the dynamics of muzzle blast development between firings from defect-free and worn barrels. The obtained results served as a basis for developing a barrel condition classifier based on muzzle blast video recordings. A methodology for analyzing synchronized video streams was developed.

The analysis identified informative features that distinguish muzzle blasts from defect-free and worn barrels. This allowed the development of a binary classifier based on least squares support vector machines (LSSVM). To assess classification quality, in addition to first- and second-type classification errors, an integral performance metric – the probability of error-free classification – was proposed. It was established that, for the experimental dataset, the classification errors based on the analysis of muzzle blast video recordings are: the first-type error $F_1 = 0.33$; the second-type error $F_2 = 0.15$; probability of error-free classification $P_0 = 0.52$.

A concept for a universal barrel condition classifier was proposed. The concept involves classification based on both muzzle blast video recordings and the acoustic fields of the shot – ballistic and muzzle waves. It was shown that, in this case, the probability of error-free classification increases to 0.77. The proposed concept made it possible to develop and investigate an automated system for diagnosing shot condition parameters.

Conflict of interest

The authors declare that they have no conflict of interest in relation to this research, whether financial, personal, authorship or otherwise, that could affect the research and its results presented in this paper.

Use of artificial intelligence statement

Artificial intelligence technology was used in the preparation of this chapter. Specifically, the authors used OpenAI ChatGPT (model GPT-5.2) to assist in editing and structuring introductory text sections and in formulating generalized descriptions of research methodologies for integrating mandatory literature sources into the chapter introduction.

The authors bear full responsibility for the final manuscript. Generative AI tools are not credited and are not responsible for the final results.

Authors' contributions

Volodymyr Demidenko: Conceptualization, Methodology, Experimental design, Integration of acoustic and visual data, Writing – original draft.

Yevhenii Dobrynin: Data processing, Feature extraction, Development of classification algorithms, Validation of results.

Maksym Maksymov: Analysis of synchronized measurement channels, Performance assessment, Interpretation of results.

Ruslan Riaboshapka: Visualization of results, Technical support of experiments, Writing – review & editing.

References

1. Boltenkov, V., Brunetkin, O., Dobrynin, Y., Maksymova, O., Kuzmenko, V., Gultsov, P. et al. (2021). Devising a method for improving the efficiency of artillery shooting based on the Markov model. Eastern-European Journal of Enterprise Technologies, 6 (3 (114)), 6–17. https://doi.org/10.15587/1729-4061.2021.245854
2. Dobrynin, Y., Volkov, V., Maksymov, M., Boltenkov, V. (2020). Development of physical models for the formation of acoustic waves at artillery shots and study of the possibility of separate registration of waves of various types. Eastern-European Journal of Enterprise Technologies, 4 (5 (106)), 6–15. https://doi.org/10.15587/1729-4061.2020.209847
3. Dobrynin, Y., Brunetkin, O., Maksymov, M., Maksymov, O. (2020). Constructing a method for solving the riccati equations to describe objects parameters in an analytical form. Eastern-European Journal of Enterprise Technologies, 3 (4 (105)), 20–26. https://doi.org/10.15587/1729-4061.2020.205107
4. Brunetkin, O., Beglov, K., Brunetkin, V., Maksymov, O., Maksymova, O., Havaliukh, O., Demydenko, V. (2020). Construction of a method for representing an approximation model of an object as a set of linear differential models. Eastern-European Journal of Enterprise Technologies, 6 (2 (108)), 66–73. https://doi.org/10.15587/1729-4061.2020.220326
5. Brunetkin, O., Maksymov, M., Brunetkin, V., Maksymov, O., Dobrynin, Y., Kuzmenko, V., Gultsov, P. (2021). Development of the model and the method for determining the influence of the temperature of gunpowder gases in the gun barrel for explaining visualize of free carbon at shot. Eastern-European Journal of Enterprise Technologies, 4 (1 (112)), 41–53. https://doi.org/10.15587/1729-4061.2021.239150
6. Brunetkin, O., Maksymov, M., Dobrynin, Y., Demydenko, V., Sidelnykov, O. (2024). Development of a process model for determining the composition and energy characteristics of a pyrotechnic mixture using the library method. EUREKA: Physics and Engineering, 5, 99–112. https://doi.org/10.21303/2461-4262.2024.003453

7. Brunetkin, O., Dobrynin, Y., Maksymenko, A., Maksymova, O., Alyokhina, S. (2020). Inverse problem of the composition determination of combustion products for gaseous hydrocarbon fuel. Computational Thermal Sciences: An International Journal, 12 (6), 477–489. https://doi.org/10.1615/computthermalscien.2020034878
8. Maksymov, M. V., Brunetkin, O. I., Beglov, K. V., Alyokhina, S. V., Butenko, O. V. (2022). Automatic Control for the Slow Pyrolysis of Organic Materials with Variable Composition. Advanced Control Systems: Theory and Applications. Series in Automation, Control and Robotics. River Publishers, 397–434. https://doi.org/10.1201/9781003337010-16
9. Brunetkin, O. I., Beglov, K. V., Maksymov, M. M., Ulytska, O. O. (2021). Model and method of controlled pyrolysis of organic substances of variable composition. Problems of Control and Informatics, 66 (1), 134–146. https://doi.org/10.34229/1028-0979-2021-1-12
10. Brunetkin, O., Sidelnykov, O., Maksymov, M., Dobrynin, Y. (2025). Improving the model for determining the composition of gunpowder gases during thermal destruction of gunpowder in a limited volume space. Eastern-European Journal of Enterprise Technologies, 3 (6 (135)), 35–45. https://doi.org/10.15587/1729-4061.2025.330654
11. Dobrynin, Y., Maksymov, M., Boltenkov, V. (2020). Development of a method for determining the wear of artillery barrels by acoustic fields of shots. Eastern-European Journal of Enterprise Technologies, 3 (5 (105)), 6–18. https://doi.org/10.15587/1729-4061.2020.206114
12. Dobrynin, Y. V., Boltenkov, V. O., Maksymov, M. V. (2020). Information technology for automated assessment of the artillery barrels wear based on SVM classifier. Applied Aspects of Information Technology, 3 (3), 117–132. https://doi.org/10.15276/aait.03.2020.1
13. Suykens, J. A. K., Van Gestel, T., De Brabanter, J., De Moor, B., Vandewalle, J. (2002). Least Squares Support Vector Machines. Singapore: World Scientific, 295. https://doi.org/10.1142/5089
14. Xia, X.-L., Jiao, W., Li, K., Irwin, G. (2013). A Novel Sparse Least Squares Support Vector Machines. Mathematical Problems in Engineering, 2013, 1–10. https://doi.org/10.1155/2013/602341
15. LS-SVMlab toolbox. Available at: https://www.esat.kuleuven.be/sista/lssvmlab/
16. James, G., Witten, D., Hastie, T., Tibshirani, R. (2013). Support Vector Machines. An Introduction to Statistical Learning. New York: Springer, 337–372. https://doi.org/10.1007/978-1-4614-7138-7_9